



Share Your Innovations through JACS Directory

Journal of Nanoscience and Technology

Visit Journal at <http://www.jacsdirectory.com/jnst>

Improved Performance of Natural Dye for Eco-friendly Solar Cell Application using SnO₂ Nanoparticles by Chemical Precipitation Method

P. Backialakshmi, C. Gopinathan*

Department of Solar Energy, School of Energy Sciences, Madurai Kamaraj University, Madurai – 625 021, Tamil Nadu, India.

ARTICLE DETAILS

Article history:

Received 14 May 2018

Accepted 25 May 2018

Available online 30 May 2018

Keywords:

SnO₂ Photoelectrode*Curcuma longa*

Natural Dye

ABSTRACT

Natural dye-sensitized solar cells (NDSSCs) have gained important interest in the field of solar energy owing to their low production cost, simple fabrication and good efficiency. In the present study, SnO₂ nanoparticles were prepared by chemical precipitation method. The photoanode is fabricated using doctor-blade technique. In this paper, the dye molecules absorb light and make excited electrons the technique adopted, which in revolve create current in the output terminals of the cell. Graphite coated glass was used as the counter electrode. The prepared nanoparticles are characterized by powder X-ray diffraction (XRD), scanning electron microscopy (SEM), energy dispersive X-ray spectroscopy (EDX), and UV-Visible spectroscopy. XRD analysis confirms the structure of tetragonal structure with rutile phase, and crystallite sizes 20-30 nm. *Curcuma longa* dye extract used as photosensitizer. FTIR results show the M-O (Sn-O) bond with no other distinct impurities from the chemical reactions that were used for SnO₂ preparation. Finally, photocurrent-voltaic characterization of nano-crystalline natural dye solar cell using I-V studies. It was found that the levels of short-circuit current (J_{sc}), open-circuit voltage (V_{oc}), fill factor (FF) and overall conversion efficiency (η) of *Curcuma longa* dye extract. Further suggestions to improve the efficiency of NDSSC are discussed.

1. Introduction

Solar cells are very gifted for directly converting solar energy into electric energy without pollution, sound, or moving parts. The growth of energy generation from solar cells is significantly increased and becoming the best with all the renewable technologies [1]. As the third generations of solar cells, dye-sensitized solar cells (DSSCs) are low cost and simple manufacturing when compared to silicon-based solar cells. Moreover, DSSCs are attracting great research interests, especially how to improve performance and stability [2]. However, improving the efficiency of DSSCs is not a simple task as there are a lot of variables and many layers involved. Two main key layers that are researched and still require to be optimized are semiconductor photoanodes and dyes. Both are a sensitizer for absorbing ultraviolet and visible lights [3-5], a generator for charge carriers, and transporter electrons into the layer of transparent conductive oxide. An example of text Dispersing nanoparticles smaller than 100 nm of diameter into water, ethylene glycol, engine oil, and other base fluids was defined as nanofluid [1]. Most of the earlier literature reported that adding of nanoparticles into base fluid enhances the convective heat transfer presentation. Owing to the attendance of nanoparticles, the thermophysical of nanofluids can dramatically change such as the increased thermal conductivity, density, and also viscosity, and the reduced specific heat without severe sedimentation [2, 3]. Another function of semiconductor photo-anodes is to adsorb dyes. Strong dye adsorption on the semiconductor photo-anode surface is required for efficient DSSCs [6, 7]. The adsorption capability is affected by immersing time, dye concentration, dye acidity, immersing temperature, solvent, semiconductor size, and semiconductor porosity.

Up till now TiO₂ is the best understood and successful anode material prototype in DSCs owing to its good chemical stability, high density of states in its conduction band, and suitable band alignment and electronic coupling with a great range of organic and inorganic dyes. However, the rather low electron mobility through nanocrystalline nanoporous TiO₂ photoanodes (ca. 0.1 cm²V⁻¹s⁻¹) and the photocatalytic activity of anatase titania have led to crucial limitations both in terms of further performance improvement and long-term stability of the cells. Along with zinc oxide

(ZnO) [8], tetragonal tin dioxide (SnO₂) is a promising alternative functional material to be used as a photoanode in DSSCs [9] owing to its larger bandgap (3.6 eV), more positive conduction band making it for a better electron acceptor and much higher electron mobility both as bulk (ca. 240 cm²V⁻¹s⁻¹) [10] and as a nanocrystalline material (ca. 125 cm²V⁻¹s⁻¹) [11]. As an effect, faster electron collection and better long-term stability under illumination of the corresponding devices should be conceptually achieved by using SnO₂-based electrodes.

All these studies employ low-cost natural dye, eco-pleasant however they still utilize an expensive metal such as platinum (Pt) as a counter electrode owing to its high catalytic activity. Though, a few information have claimed that platinum gets decomposed with triiodide containing electrolytes and forms platinum iodides such like PtI₄ [12, 13]. Large-scale solar energy conversion systems involve in abundance obtainable low-cost materials in the long run and so there is a need to investigate a counter electrode that is less costly and noncorrosive in electrolyte [14, 15]. In this investigation, we have used graphite as a counter electrode in order to reach this goal.

In this manuscript we reported synthesis of SnO₂ nanoparticles using chemical precipitation method. The synthesized nanoparticles were employed for DSSC application using doctor-blade techniques. So, future, there have been a very few reports on DSSC applications by natural dye extract. In this study, we report the interesting natural dye is extracted from turmeric roots with using graphite as a counter electrode which are cheap and available. Unfortunately, the efficiency of DSSCs with turmeric-platinum based DSSC from previous studies is still low, i.e. 0.264% [16], 0.6% [17], 0.63% [18], and 0.03% [19]. To the best of our knowledge, this work constitutes the first example of SnO₂-based photoanodes for DSSC application using turmeric natural dye-graphite coated counter electrode showing both enhanced photoconversion efficiency and long-term stability in DSSC.

2. Experimental Methods

2.1 Materials

All chemical reagents were procured with AR purity, and used directly without further purification. SnCl₄·5H₂O, ammonia, and H₂O₂ were purchased from Sigma Aldrich. Using chemical precipitation method SnO₂

*Corresponding Author: cgnmku64@gmail.com (C. Gopinathan)

samples were prepared according to the reported procedures in the literatures [20]. The materials used in this experiment were fluorine tin oxide (FTO) coated glass plate (Dyesol, Australia), Triton X-100 (Merck, Germany), ethanol (Germany) and acetone (Germany), dye extracted from turmeric, graphite, potassium iodide, iodine and acetonitrile.

2.2 Preparation of SnO₂ Particles

In chemical co-precipitation method, SnO₂ nanoparticles were prepared using dissolving 1 g stannous chloride dehydrates in 100 mL distilled water. After complete finish, 4 mL ammonia solution was added to the above solution by drop wise under stirring. Further the solution was stirred for 2 h, and then few drops of H₂O₂ were added while stirring until the solution changed its color. The result was then washed and filtered two times, finally, calcined at 500 °C for 2 h. The calcinations temperature was used 500-600 °C because modifications of SnO to SnO₂ by direct heating [21].

2.3 Electrode Preparation

The synthesized SnO₂ nanoparticles (1 g) were ground in a porcelain mortar with 0.5 mL of water containing 50 µL of acetylacetone till getting a viscous paste followed by slow addition of 2.5 mL of water and 20 µL of Triton X-100 under continuous grinding. From this colloidal mixture, photoanode (0.25 cm² area) was prepared on a FTO conducting glass (Pilkington, TEC-7, ~6 ~ 8 ohms/square) using doctor-blade technique. The film was then dried and sintered at 450 °C in a muffle furnace for 30 min and allowed to cool upto 80 °C.

2.4 Soaking of Electrode

Fig. 1 shows the SnO₂ coated glass plate which was soaked in turmeric dye for 24 h in dark and sealed place. Then glass plate was washed using ethanol and dried in air for few minutes.

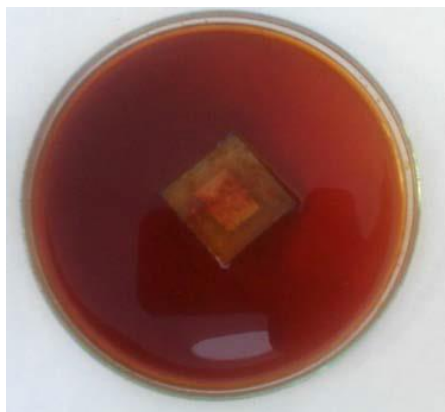


Fig. 1 Photograph of turmeric dye dipped SnO₂ coated on FTO glass

2.5 Electrolyte Preparation

Electrolyte was prepared by mixing 0.127 g (0.05 M) of iodine and 0.83 g (0.5 M) potassium iodide in 10 mL ethylene glycol. The electrolyte solution was stored in a black bottle by wrapping with aluminum foil.

2.6 Graphite Coated Counter Electrode

Fig. 2 shows the graphite coated counter electrode. To make the counter (positive) electrodes, the conducting side of the uncoated FTO plates were coated with help of the soft pencil to spread the entire conductive side of the FTO plate.



Fig. 2 Graphite coated counter electrode

<https://doi.org/10.30799/jnst.121.18040309>

Cite this Article as: P. Backialakshmi, C. Gopinathan, Improved performance of natural dye for eco-friendly solar cell application using SnO₂ nanoparticles by chemical precipitation method, J. Nanosci. Tech. 4(3) (2018) 402–406.

2.7 Preparation of Dye Sensitizer Solutions

Fig. 3 shows natural dye of turmeric extract. Curcumin was extracted from commercially purchased turmeric powder prepared from the ground rhizome of *Curcuma longa* L. Approximately 0.25 g of the sample was dissolved in 50 mL of ethanol. The extractants were properly stored, protected from direct sunlight, and used further as sensitizers in DSSCs [22].



Fig. 3 Natural dye of turmeric extract

2.8 Cell Fabrication

Fig. 4 shows image of dye sensitized solar cells. Electrode and counter electrode were joint mutually keeping SnO₂ paste coated surface and the graphite coated surface face to face. Few drops of electrolyte solution was given in the contact of two glasses and by the capillary action the electrolyte was uniformly distributed throughout the stained SnO₂ film. Using cotton or tissue to remove the excess electrolyte from the exposed area of the glass. The whole cell was then taken to sunlight for illumination.

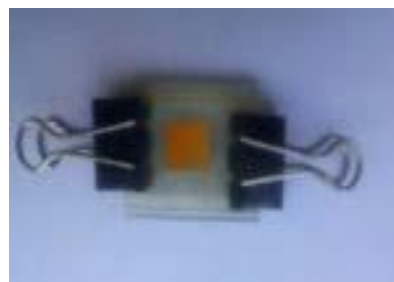


Fig. 4 Schematic diagram of dye sensitized solar cells

2.9 Principle of Operation of DSSC

Fig. 5 shows the mechanism of DSSC and total configuration of our DSSC. Under illumination of sun light energy, photon will hit through conductive layer glass; fluorine-doped tin oxide (FTO) towards dye molecules which rise on the surface of SnO₂ particles. The photon excitations of dye will basis an injection of an electron into conduction band of the SnO₂ layer. These electrons will go the external loop during the load. For the moment, dye molecule which had lost electron will be restored by electron donation from redox electrolyte (contain iodide/triiodide), which in this experiment; a combination of potassium iodide (KI) and iodine (I₂) [23]. This procedure occurs very fast avoiding any recombination of electrons discarded former. Under illumination, voltage is generated during potential difference between Fermi level of SnO₂ layer and redox electrolyte.

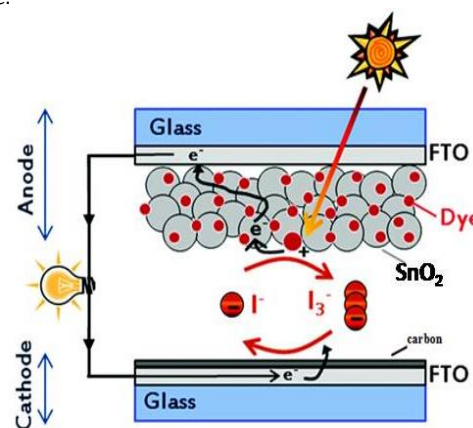


Fig. 5 Schematic representation of SnO₂ based DSSC

3. Results and Discussion

3.1 Structural Analysis

Fig. 6 shows the diffraction pattern of synthesized SnO₂ nanoparticles. The pointed and high intensity peaks in X-ray diffraction (XRD) pattern; it indicates the material with high crystallinity. From XRD pattern all the reflection peak positions can be indexed as tetragonal SnO₂ phase. While additional impurities, such as metallic Sn and other tin oxides are not observed. Though, the diffraction peaks are broadened owing to the small crystallite sizes of SnO₂.

Using Bragg's diffraction equation $2d\sin\theta = n\lambda$, where d = interplanar spacing, θ = angle of diffraction, n = order of diffraction and $\lambda = 1.54 \text{ \AA}$ (wavelength of X-ray), the 'd' values are calculated for different planes.

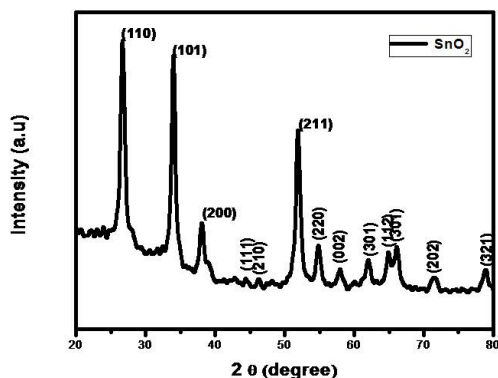


Fig. 6 XRD patterns of synthesized SnO₂ nanostructures

Table 1 gives the data for observed 'd' values and standard 'd' values from JCPDS file No.: 41-1445 for tetragonal SnO₂ phase. The observed 'd' values are found to be matching with standard 'd' values indicating thereby the formation of single SnO₂ phase with tetragonal symmetry. From Table 1. Data for observed 'd' values and standard 'd' values from JCPDS file no.: 41-1445 for tetragonal SnO₂ phase.

Table 1 XRD parameters of SnO₂ nanoparticles

S.No.	hkl	2θ	θ	sinθ	2sinθ	Standard d (Å)	Observed d (Å)
1.	110	26.36	13.18	13.18	0.45	3.35	3.37
2.	101	33.82	16.91	16.91	0.58	2.65	2.64
3.	200	37.70	18.85	18.85	0.64	2.37	2.3
4.	211	51.52	25.76	25.76	0.86	1.76	1.77

Scherrer's formula $D = 0.9\lambda/\beta\cos\theta$, where D is crystallite size, β is FWHM of the observed peak, λ is wavelength of the X-ray and θ is angle of diffraction, is used to estimate average crystallite size, of SnO₂ samples prepared, using its (110), (101), (200) and (211) orientations.

Table 2 The mean crystallite size in different crystallography orientation form XRD pattern

S.No.	hkl	2θ	FWHM	Crystallite size (nm)
1.	110	26.36	0.64	22
2.	101	33.6	0.49	29
3.	200	37.70	0.60	24
4.	211	51.52	0.52	29

The calculated crystallite size of SnO₂ from Table 2 is in the range of 20–30 nm. The smallest crystallite size has largest specific surface area, which will be helpful for more dye adsorption and will help to enhance photovoltaic performance of the cell made of this.

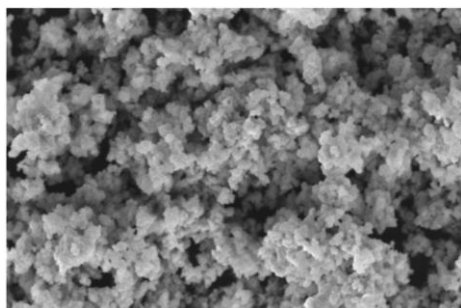


Fig. 7 SEM image of SnO₂ nanostructure
<https://doi.org/10.30799/jnst.121.18040309>

3.2 Surface Morphological Analysis

The sponge-like structure in SEM image of the top view of SnO₂ film coated on TCO electrode is shown in Fig. 2. The film is about 12 μm thick and the spherical SnO₂ nanoparticles are homogeneously spread within the SnO₂ layer it shows like flower. No rupture on the surface and no gaps between the coatings were observed, it represent, brilliant inter-particle connectivity and inter-layer attachment.

3.3 Optical Properties

Fig. 8 shows the optical absorption spectra of synthesized SnO₂ photoanodes. A broad absorption edge in the ultraviolet region near ~355 nm is observed, which corresponds to a typical rutile SnO₂ absorption edge in the UV region. This peak usually occurs owing to the charge-transfer from the valence band to the conduction band of SnO₂. The resultant band gap energy is predictable from the graph of $(\text{Absorbance})^2$ vs. $h\nu$ and is shown in Fig. 9. The band gap observed band gap is 3.64 eV. The experimental band gap is higher than the reported band gap of bulk SnO₂. The observed higher band gap of the SnO₂ confirms the structure of nanocrystalline nature of SnO₂. The increase in band gap of SnO₂ is too related to the porosity of the film [24, 25].

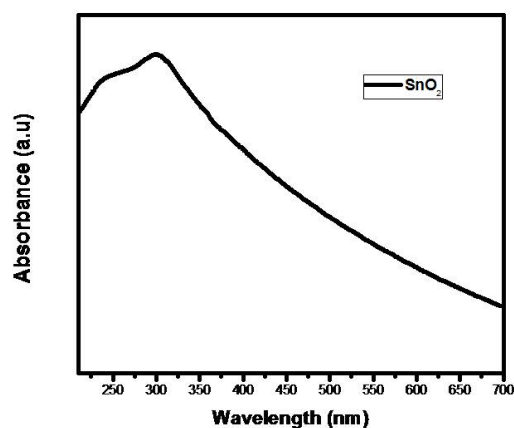


Fig. 8 Absorption spectra of SnO₂ nanoparticles

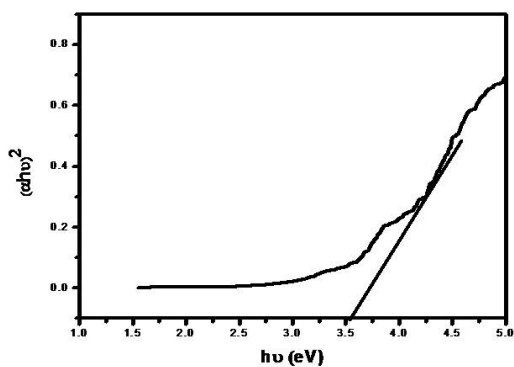


Fig. 9 Plot of $(\alpha h\nu)^2$ vs. photon energy ($h\nu$) for SnO₂

3.4 FTIR Analysis

FTIR spectrum is recorded in the region 4000–400 cm⁻¹. Fig. 10 shows the FTIR spectra of SnO₂ samples synthesized SnO₂ samples. A high intense and broad band in the range of 3500 to 3200 cm⁻¹ is assigned to O-H stretching of water molecule adsorbed on the surface of SnO₂ [26–33]. The major IR peaks corresponding to Sn-O and O-Sn-O bond vibrations appear in the range of 700–400 cm⁻¹. The strong peak appeared at 620 cm⁻¹ can be assigned to Sn-O-Sn [34]. The presence of vibration peaks attributed to Sn-O bond vibration confirms the formation of SnO₂.

Fig. 11 shows the IR spectra of curcumin. The spectrum of curcumin in the present study coincides with that reported by Zebib et al., [35]. The broad band at 3341 cm⁻¹ was assigned to the vibrations of the free hydroxyl-group of phenol (Ar-OH). The bands at 719, 815 and 962 cm⁻¹ were attributed to the bending vibrations of the C-H bond of alkene groups (RCH=CH₂). An intense band at 1745 cm⁻¹ assigned to the vibration of the carbonyl bond (C=O) accompanied by a small shoulder at 1712 cm⁻¹ was attributed to the Keto-enol tautomerism of curcumin. The bands at 1463 and 1378 cm⁻¹ corresponding to the vibrational mode of C-O elongation of the alcohol and phenol groups confirmed the extraction of curcumin from turmeric.

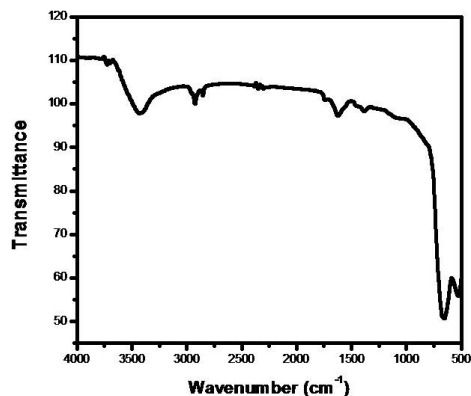


Fig. 10 FTIR patterns of Synthesized SnO₂ nanoparticles

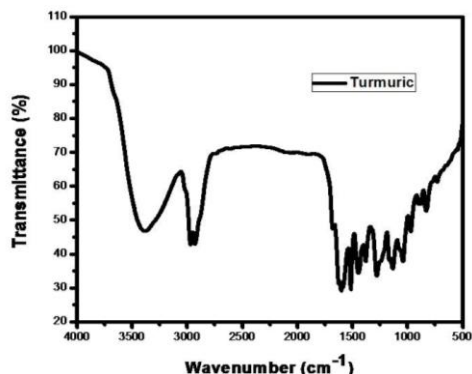


Fig. 11 FT-IR spectrum of natural dye extracted from *Curcuma longa* L.

3.5 Performance of Fabricated Cell

Photovoltaic tests of the fabricated DSSCs using these natural dye as sensitizers and graphite coated counter electrode were performed by measuring the I-V curve of cell under irradiation with white light (100 mW/cm²) from xenon arc lamp and at room temperature (22.3° C with cell area 0.25 cm²). The values of fill factor (FF) was calculated by applying the following generalized equation $FF = P_{max}/I_{sc}V_{oc}$, where V_{oc} and I_{sc} respectively the open circuit voltage and short circuit current; P_{max} is the maximum power delivering point. The I-V characteristics of the prepared DSSCs taking turmeric dye, as the natural dye by using Doctor-blade with SnO₂ nanoparticles is shown in Fig. 12. The photoelectric conversion efficiency (η) of DSSC is given as $\eta = (I_{sc}V_{oc}/P_{in}) \times FF$, where P_{in} is the incident light power.

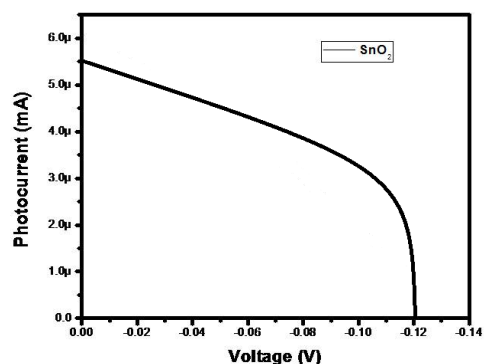


Fig. 12 I-V measurements of SnO₂ nanoparticles

Table 3 I-V parameters of SnO₂ nanoparticles

S.No	SnO ₂ Photoanode	J_{sc} (Acm ⁻²)	V_{oc} (V)	J_{max} (Acm ⁻²)	V_{max} (V)	FF	$\eta\% \times 10^{-2}$
1.	using turmeric extract	2.55×10^{-4}	0.85	1.58×10^{-4}	0.505	0.455	0.039

Table 3 shows the data acquired from measuring the photoelectric conversion efficiency of the DSSCs. The DSSC output power was calculated using the I-V data. Fig. 12 shows the power as a function of V for the DSSC sensitized by turmeric dye extract. According to Sreekala et al. [36] a better photovoltaic performance was obtained when the curcumin dye was extracted with acetone as a solvent, they obtained efficiency; open circuit voltage (V_{oc}), short circuit current density and fill factor of 0.63%, 0.43 V, 1.35 mA cm⁻² and 0.517, respectively. In the present study, using <https://doi.org/10.30799/jnst.121.18040309>

ethanol as the extractant, using graphite an counter electrode the efficiency, V_{oc} , current density and fill factor was 0.039%, 0.50 V, 2.58 mA cm⁻² and 0.088, respectively.

4. Conclusion

In summary, using chemical precipitation method tetragonal structured tin oxide nanoparticles were synthesized. Graphite coated FTO used a counter electrode, natural dye extracted from the turmeric used a photosensitizer and liquid electrolyte KI₃ were used to assemble DSSCs. Natural dyes as another sensitizers for DSSCs are predictable to be promising because of several reasons such as the effortless preparation technique and little charge. The SEM picture of the SnO₂ film shows that the nanoparticles are non-homogeneous and has a spongy agglomerate structure consisting mainly of spherical crystalline particles. While the efficiency of the using natural dye and graphite coated counter electrode on SnO₂NPs based liquid-state DSSCs is low, we trust that the performance of these cells can be better further with employing an efficient dye-sensitizer.

References

- [1] J. Gong, J. Liang, K. Sumathy, Review on dye-sensitized solar cells (DSSCs): Fundamental concepts and novel materials, *Renew. Sust. Ener. Rev.* 16(8) (2012) 5848-5860.
- [2] T. Suyitno, J. Saputra, A. Supriyanto, Z. Arifin, Stability and efficiency of dye-sensitized solar cells based on papaya-leaf dye, *Spectrochim. Acta Mol. Biomol. Spectrosc.* 148 (2015) 99-104.
- [3] K. Wongcharee, V. Meeyo, S. Chavadej, Dye-sensitized solar cell using natural dyes extracted from rosella and blue pea flowers, *Sol. Energy. Mat. Sol. Cells* 91 (2007) 566-571.
- [4] S. Tekerek, A. Kudret, U. Alver, Dye-sensitized solar cells fabricated with black raspberry, black carrot and rosella juice, *Ind. J. Phys.* 85 (2011) 1469-1476.
- [5] H. Chang, H.M. Wu, T.L. Chen, K.D. Huang, C.S. Jwo, Y.J. Lo, The effect of electrolyte on dye sensitized solar cells using natural dye from mango (*M. indica* L.) leaf as sensitizer, *J. Alloys Compd.* 495 (2010) 606-610.
- [6] N.A. Ludin, A.M.A.A. Mahmoud, A.B. Mohamad, A.A.H. Kadhum, K. Sopian, N.S.A. Karim, Review on the development of natural dye photosensitizer for dye-sensitized solar cells, *Renew. Sust. Ener. Rev.* 31 (2014) 386-396.
- [7] Y. Ooyama, Y. Harima, Photophysical and electrochemical properties, and molecular structures of organic dyes for dye-sensitized solar cells, *Chem. Phys. Chem.* 13(18) (2012) 4032-4080.
- [8] M. Saito, S. Fujihara, Large photocurrent generation in dye-sensitized ZnO solar cells, *Energy Environ. Sci.* 1 (2008) 280-286.
- [9] T. Toupance, H. El Hamzaoui, B. Jousseume, H. Riague, I. Saadeddin, G. Campet, J. Brotz, Bridged polystannoxane: a new route toward nanoporous tin dioxide, *Chem. Mater.* 18 (2006) 6364-6372.
- [10] Z.M. Jarzelski, J.P. Marton, SnO₂ dense ceramic microwave sintered with low resistivity, *J. Electrochem. Soc.* 123 (1976) 299C-310C.
- [11] M.S. Arnold, P. Avouris, Z.W. Pan, Z.L. Wang, Field-effect transistors based on single semiconducting oxide nanobelts, *J. Phys. Chem. B* 107 (2003) 659-663.
- [12] E. Olsen, G. Hagen, S.E. Lindquist, Dissolution of platinum in methoxy propionitrile containing LiI/I₂, *Sol. Ener. Mater. Sol. Cells* 63 (2000) 267-273.
- [13] G. Veerappan, K. Bojan, S.W. Rhee, Sub-micrometer-sized graphite as a conducting and catalytic counter electrode for dye-sensitized solar cells, *ACS Appl. Mater. Interf.* 3 (2011) 857-862.
- [14] Z. Huang, X. Liu, K. Li, D. Li, Y. Luo, H. Li, Application of carbon material as counter electrodes of dye sensitized solar cell, *Electrochem. Commun.* 9 (2007) 596-598.
- [15] J.D. Roy-Mayhew, D.J. Bozym, C. Punckt, I.A. Aksay, Functionalized graphene as a catalytic counter electrode in dye-sensitized solar cells, *ACS Nano.* 4 (2010) 6203-6211.
- [16] B. O'Ragan, M. Gratzel, A low-cost, high efficiency solar cell based on dyesensitized colloidal TiO₂ films, *Nature* 353 (1991) 737-740.
- [17] H.J. Kim, D.J. Kim, S.N. Karthick, K.V. Hemalatha, C.J. Raj, S. Ok, Curcumin dye extracted from *Curcuma longa* L. used as sensitizers for efficient dye-sensitized solar cells, *Int. J. Electrochem. Sci.* 8 (2013) 8320-8328.
- [18] C. Sreekala, I. Jinchu, K. Sreelatha, Y. Janu, N. Prasad, M. Kumar, Influence of solvents and surface treatment on photovoltaic response of DSSC based on natural curcumin dye, *IEEE J. Photovolt.* 2(3) (2012) 312-319.
- [19] S. Suhaimi, M.M. Shahimin, I.S. Mohamad, M.N. Norizan, Comparative study of natural anthocyanins compound as photovoltaic sensitizer, *Adv. Environ. Biol.* 7(12) (2013) 3617-3620.
- [20] N.N. Asama, S.N. Azhar, M.S. Abdulla, Preparation and characterization of SnO₂ nanoparticles, *Int. J. Innov. Res. Sci. Eng. Technol.* 2(12) (2013) 7068-7072.
- [21] R. Rammamorthy, M.K. Kennedy, H. Nienhaus, Surface oxidation of monodisperse SnO_x nanoparticles, *Sens. Actuat. B* 88 (2002) 281-285.
- [22] H.J. Kim, D.J. Kim, S.N. Karthick, K.V. Hemalatha, C. Justin Raj, Curcumin dye extracted from *Curcuma longa* L. used as sensitizers for efficient dye-sensitized solar cells, *Int. J. Electrochem. Sci.* 8 (2013) 8320-8328.
- [23] M. Gratzel, Dye-sensitized solar cell, *J. Photochem. Photobiol. C* 4 (2003) 145-153.
- [24] L.E. Brus, Electron-electron and electron-hole interactions in small semiconductor crystallites: The size dependence of the lowest excited electronic state, *J. Chem. Phys.* 80(9) (1984) 4403-4409.
- [25] A. Mortezaali, S.R. Sani, F.J. Jooni, Correlation between porosity of porous silicon and optoelectronic properties, *J. Non-Oxide Glass* 1 (2009) 293-299.

- [26] M. Krishna, S. Komarneni, Conventional vs. microwave-hydrothermal synthesis of tin oxide, SnO₂ nanoparticles, *Ceram Int.* 35 (2009) 3375–3379.
- [27] L.C. Nehru, V. Swaminathan, C. Sanjeeviraja, Rapid synthesis of nanocrystalline ZnO by a microwave- assisted combustion method, *Powder Technol.* 226 (2012) 29–33.
- [28] M. Ristic, M. Ivanda, S. Popovic, Svetozar Music, Dependence of nanocrystalline SnO₂ particle size on synthesis route, *J. Non-Cryst. Solids* 303 (2002) 270–280.
- [29] J.J. Wu, S.C. Liu, Catalyst-free growth and characterization of ZnO nanorods, *J. Phys. Chem. B* 106 (2002) 9546–9551.
- [30] B.C. Smith, *Infrared spectral interpretation: a systematic approach*, CRC Press, Boca Raton, 1998.
- [31] S. Gnanam, V. Rajendran, Luminescence properties of EG-Assisted SnO₂ nanopartilces by sol-gel process, *Dig. J. Nanomater. Bios.* 5 (2010) 699–704.
- [32] S.A. Ahmed, Room-temperature ferromagnetism in pure and Mn doped SnO powders, *Solid State Commun.* 150 (2010) 2190–2193.
- [33] B. Behera, P. Nayaka, R.N.P. Choudhary, Impedance spectroscopy study of NaBa₂V₅O₁₅ ceramic, *J. Alloys Compd.* 436 (2007) 226–232.
- [34] D.C. Sinclair, A.R. West, Impedence and modulus spectroscopy of semiconducting BaTiO₃ showing positive temperature coefficient of resistance, *J. Appl. Phys.* 66 (1989) 3850–3856.
- [35] B. Zebib, Z. Mouloungui, V. Noirot, Stabilization of curcumin by complexation with divalent cations in glycerol/water system, *Bioinorg. Chem. Appl.* 2010 (2010) 292760–1–8.
- [36] C.O. Sreekala, I. Jinchu, K.S. Sreelatha, Y. Janu, N. Prasad, M. Kumar, et al., Influence of solvents and surface treatment on photovoltaic response of DSSC based on natural curcumin dye, *IEEE J. Photovolt.* 2 (2012) 312–319.